Continuum Mech. Thermodyn.
https://doi.org/10.1007/s00161-024-01329-w

ORIGINAL ARTICLE

Yuriy Pyr'yev · **Larry Murcia Terranova**

Vibration analysis associated with the operation of printing units in offset printing machines: applications towards metamaterials

Received: 28 June 2024 / Accepted: 30 August 2024

Abstract The paper analyzes the vibrational behavior of cylinders in the offset printing machine caused by a cylinder gap shock. Specifically, it assesses the stability of a system of two cylinders. The analysis of the proposed model is reduced to solving a set of Hill equations. The singularity of the obtained equations is the relationship between the natural frequencies of the system and modulation depth. Numerical simulations, along with the generalized Hill's determinant method, were employed to determine the critical parameters of parametric resonance, thereby establishing the conditions necessary for the stability of periodic vibrations.

Keywords Parametric vibrations · Hill equations · 2DoF system · Analysis of stability

1 Introduction

The presence of vibrations of offset printing machines is a serious problem that can cause issues with the course of the printing process and reduce the quality of obtained prints. The most significant cause of vibrations of offset machines is the construction of printing units, whose main components are three cylinders (Fig. 1a): plate, blanket and impression cylinder.

Two of them—the plate cylinder and blanket cylinder—are in direct contact, and the various phenomena occurring during their turns can be a source of vibration. According to the literature, the formation of vibrations of cylinders is connected with their design.

In [1], the author mentions the phenomenon known as "cylinder gap shock", which is associated with sudden and temporary loss of contact between the plate cylinder and the blanket cylinder, which arises as a result of turning ducts contained in both cylinders. Positions [2–4] also contain references to the problem of cylinder gap shock and describe vibrations of cylinders or the entire structure of the printing machine.

The literature on the subject of vibrations of printing machines is not extensive [5–7]. A few works related to this issue are focused on modelling of dynamic phenomena occurring in structural frames of machines [3] or in cylinders of the printing unit [2–4,8–14]. One of the main problems arising as a result of vibrations generated during the operation of the printing machine is the phenomenon of banding, which appears on the prints in the form of lighter and darker strips that are parallel to the axis of the cylinder. This phenomenon is especially noticeable on surfaces that are evenly covered with paint, i.e., uniform-colour backgrounds (full fields, completely covered with paint) or tints (fields that are not fully covered with paint). A number of scientific publications list the poor condition of the machine [2,15] and the phenomenon known as cylinder

Y. Pyr'yev
Department of Printing Technologies, Faculty of Mechanical and Industrial Engineering, Institute of Mechanics and Printing, Warsaw University of Technology, 2 Konwiktorska Street, 00-217 Warsaw, Poland

L. M. Terranova (✉)
Department of Information Engineering, Computer Science and Mathematics, Università dell'Aquila, L'Aquila, Italy
E-mail: larry.murciaterranova@graduate.univaq.it

Published online: 21 September 2024

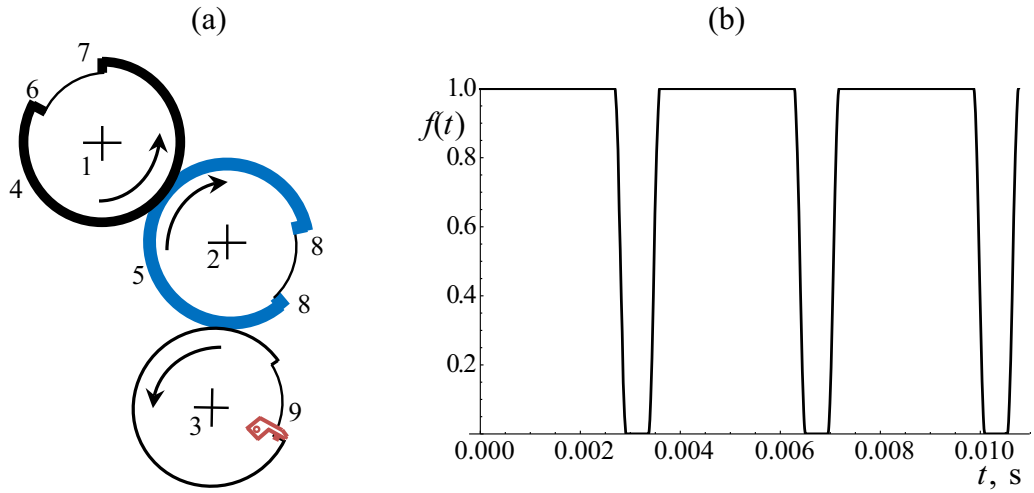

Fig. 1 **a** Turning ducts of printing cylinders; 1—plate cylinder, 2—blanket cylinder, 3—impression cylinder, 4—printing plate, 5—blanket, 6, 7—rear and front clip, 8—clips of the blanket, 9—gripper of the impression cylinder and **b** the accompanying changes in stiffness for $\varepsilon = \mathrm{T}/16$, $\varepsilon_0 = \mathrm{T}/8$, $T = 2\pi/\omega\omega = 1751.52\ s^{-1}$

gap shock (CGS) as a few causes of banding [2]. This phenomenon is a stroke occurring between the plate cylinder and the blanket cylinder, which is generated when the cylinders are turning [1,3].

However, in the literature, one can also find references to the formation of cylinder gap shock between the blanket cylinder and the impression cylinder [16].

The aim of this work is to analyse vibrations caused by cylinder gap shock, as well as to develop a methodology for assessing the stability of two cylinders when they are and they are not equipped with bearer rings (Fig. 2).

We shall consider a dual mass oscillating system with the initial conditions as a dynamic model for printing cylinders of the offset printing machine. Differential equations of vibrations of a dual mass system are stored and solved in the matrix form

$$\dot{z}\,(t) = \hat{A}\,(t)\,\mathbf{z}(t),\, \mathbf{z}\,(0) = \mathbf{z}_0 \tag{1}$$

where $\boldsymbol{z}(t) = [z_1, z_2,\ z_3,\ z_4]^T$ - state vector, $\hat{A}$ **-** matrix of the system.

A lot of studies have carried out analysis of forced and free vibrations of the system with two degrees of freedom for constant coefficients of the $\hat{A}_0$ matrix, for example [17–22].

The analysis of forced vibrations in the case of periodic changes in coefficients of the $\hat{A}(t)$ matrix was carried out in the following works [18,23–27].

In [13], the author conducted a study after determining dynamic forces generated by an imbalance of the plate cylinder and the blanket cylinder for specific parameters and accuracy of balance adopted for printing machines of the tower type. The vibrations of offset printing machines lead to a reduction in performance and deterioration in print quality. The authors of [4,9–12] analysed the impact of bearer rings on torsional vibrations of the plate and blanket cylinders using the method of computational experiment. The vibrations of printing machines were considered in [8,14]. The article [28] presents a study on the effect of mistakes when mounting the cylinders on the print quality and on ink film thickness.

Offset printing presses, particularly the advanced ones, use precise and high-resolution printing techniques. These capabilities can be adapted to manufacture metamaterials, which often require complex and microscale patterning. Metamaterials are engineered materials with properties not typically found in natural materials [29–39]. They can be designed to have unique properties [40–46]. The precision of offset printing can be leveraged to create the detailed structures necessary for metamaterials to exhibit their unique properties. Thus, advancing knowledge of this system to improve its performance paves the way to new applications that have been ignored until now. In particular, offset printing is a form of lithography, which is a key technique used in the creation of metamaterials. Lithographic techniques are employed to pattern the small-scale structures that give metamaterials their unusual properties, such as negative refraction, negative stiffness, or cloaking.

One of the challenges in metamaterials research and application is producing them at scale and at a reasonable cost. Offset printing, being a mature and widely-used technology, offers a scalable and potentially

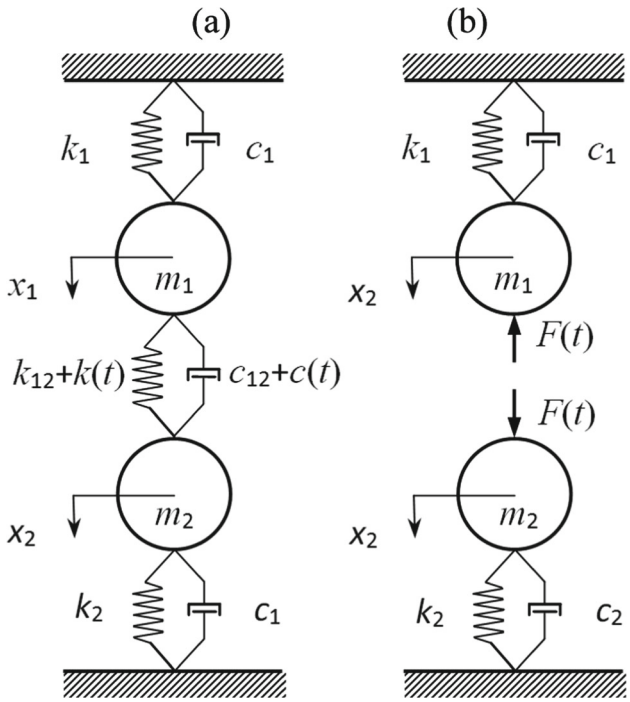

Fig. 2 Model of the printing cylinders

cost-effective method for producing metamaterial structures. This can facilitate the commercialization and practical application of metamaterials. Metamaterials have significant applications in optics, electronics, acoustics, and mechanics, areas where precise and high-quality printing techniques are crucial. Offset printing presses can be adapted to create different kinds of metamaterials, which require accurate placement and patterning of materials at the micro- or nanoscale. In summary, the advanced manufacturing capabilities of modern offset printing may be crucial in the development and production of metamaterials. The precision, scalability, and cost-effectiveness of offset printing make it a valuable technique in the field of metamaterials research and application.

The analysed system consists of a plate cylinder and blanket cylinder and has two degrees of freedom (Fig. 2).

The phenomenon of cylinder gap shock was considered as a source of parametric vibrations in the system, meaning that their formation is caused by cyclic changes in stiffness of the system associated with turning ducts (Fig. 1b).

The following study assumes that vibrations of the plate and offset cylinder take place in a vertical plane. The printing unit was reduced to the dual mass system that represents plate and blanket cylinders (Fig. 2).

2 Mathematical statement of the problem

The analysed model of plate cylinders and blanket cylinders is shown in Fig. 1. The vibrations of cylinders are caused by turning ducts, which are equipped with locks that secure the printing plate and offset blanket.

The turning ducts lead to a cyclical (with each turn of the cylinders) and sudden change in the stiffness of the system, which induces parametric vibrations of the system that are described by equations (2).

The model shown in Fig. 2a consists of two masses m_1 and m_2, three springs with the following stiffness coefficients k_1, k_2 and k_{12}. Vibrations of the system are caused by changing stiffness $k(t)$ and viscosity of $c(t)$ of the blanket. Therefore, it may be described by the following system of parametric equations

$$\begin{cases} m_1\ddot{x}_1 + c_1\dot{x}_1 + k_1x_1 + F(t) = 0 \\ m_2\ddot{x}_2 + c_2\dot{x}_2 + k_2x_2 - F(t) = 0 \end{cases} \tag{2}$$

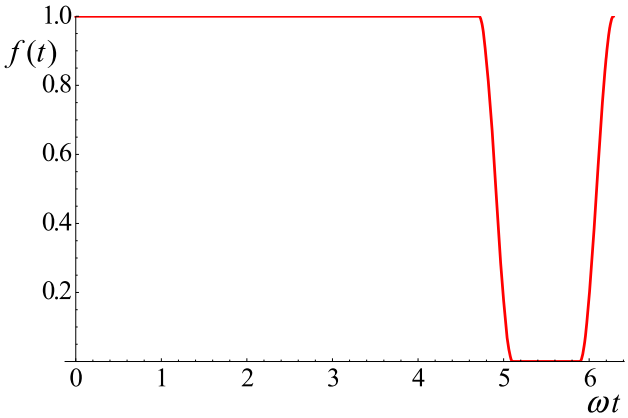

Fig. 3 Function describing a temporary decrease of the load. $\varepsilon = T/16$, $\varepsilon_0 = T/8$, $T = 2\pi/\omega$, $\omega = 1751.52\ s^{-1}$

where:

$$F(t) = k_{12}(x_1 - x_2) + c_{12}(\dot{x}_1 - \dot{x}_2) + k(t)(x_1 - x_2) + c(t)(\dot{x}_1 - \dot{x}_2) \tag{3}$$

m_1, m_2—masses of the plate cylinder and the blanket cylinder;

c_{12}, c_1, c_2 and $c(t)$ – viscous damping coefficients of dampers, which are represented by bearer rings [27], machine frame and blanket;

k_{12}, k_1, k_2 and $k(t)$ – stiffness coefficients of springs, which are represented by bearer rings [27], machine frame and offset blanket.

It is noteworthy that the periodic substructure of metamaterials in this context may be used to create a dampening effect if introduced in the linking devices modeled by k_1, k_2, c_1, and c_2. There are some trials in this regard, and to provide a few relevant examples from the literature, we refer the reader to the sources about mechanical damping, sometimes called "meta-damping" [47–49].

The changing load of cylinders arising as a result of periodic changes in stiffness and viscosity of the blanket is modelled by force (3) (Fig. 2b). More in detail, in offset printing, the initial motion is generally given to the plate cylinder, which starts the rotation and begins the process of inking the plate. As the plate cylinder rotates, the inked image is transferred to the blanket cylinder. The impression cylinder then presses the substrate against the rotating blanket cylinder, which prints the image onto the substrate. This sequence ensures that the image is accurately and consistently transferred from the plate to the substrate, a crucial aspect of high-quality offset printing. Therefore, because of the imposed motion of the plate cylinder and the periodic return of the bumping effects of the slots or gaps placed in the cylinders, periodic changes in the load of cylinders have been modelled as a periodic change in stiffness and damping of the offset blanket (3), where:

$$k(t) = kf(t), c(t) = cf(t) \tag{4}$$

$$f(t) = \begin{cases} 1, & T_n < t < T_{2\varepsilon+\varepsilon_0} \\ \tau_{\varepsilon+\varepsilon_0}^2\left(3 - 2\tau_{\varepsilon+\varepsilon_0}\right), & T_{2\varepsilon+\varepsilon_0} < t < T_{\varepsilon+\varepsilon_0} \\ 0, & T_{\varepsilon+\varepsilon_0} < t < T_\varepsilon \\ \tau_\varepsilon^2(3 + 2\tau_\varepsilon), & T_\varepsilon < t < T_{n+1} \end{cases} \tag{5}$$

$\tau_\varepsilon = (T_\varepsilon - t)/\varepsilon$, $\tau_{\varepsilon+\varepsilon_0} = (T_{\varepsilon+\varepsilon_0} - t)/\varepsilon$,

$T_{2\varepsilon+\varepsilon_0} = T_{n+1} - 2\varepsilon - \varepsilon_0$, $T_{\varepsilon+\varepsilon_0} = T_{n+1} - \varepsilon - \varepsilon_0$, $T_\varepsilon = T_{n+1} - \varepsilon$, $n = 0,1,2,...$;

$T_n = nT$, $T = 2\pi/\omega$—the period of change (decrease) in load of cylinders;

$$f(t + T) = f(t)$$

A graph of the function (5) for the exemplary parameters and for $n = 0$ is shown in Fig. 3.

Two second-order equations (2) should be reduced to four first-order equations. We will introduce new variables (state variables) according to the formulas

$$x_1 = z_1, \dot{x}_1 = z_2, x_2 = z_3, \dot{x}_2 = z_4 \tag{6}$$

obtaining an equivalent system of four first-order equations (1) instead of the (2) equation, including (7)

$$\begin{aligned}
&2h_{11} = 2h_{01} + 2h_{10}, 2h_{22} = 2h_{02} + 2h_{20}, \omega_{11}^2 = \omega_{01}^2 + \omega_{10}^2, \omega_{22}^2 = \omega_{02}^2 + \omega_{20}^2 \\
&2h_{01} = \frac{c_1}{m_1}, 2h_{02} = \frac{c_2}{m_2}, \omega_{01}^2 = \frac{k_1}{m_1}, \omega_{02}^2 = \frac{k_2}{m_2} \\
&2h_1 = \frac{c}{m_1}, 2h_2 = \frac{c}{m_2}, \omega_1^2 = \frac{k}{m_1}, \omega_2^2 = \frac{k}{m_2} \\
&2h_{10} = \frac{c_{12}}{m_1}, 2h_{20} = \frac{c_{12}}{m_2}, \omega_{10}^2 = \frac{k_{12}}{m_1}, \omega_{20}^2 = \frac{k_{12}}{m_2}
\end{aligned} \tag{7}$$

where the $\hat{A}(t)$ matrix has the following structure

$$\hat{A}(t) = \begin{bmatrix} 0 & 1 & 0 & 0 \\ -(\omega_{11}^2 + \omega_1^2 f(t)) & -2(h_{11} + h_1 f(t)) & (\omega_{10}^2 + \omega_1^2 f(t)) & 2(h_{10} + h_1 f(t)) \\ 0 & 0 & 0 & 1 \\ (\omega_{20}^2 + \omega_2^2 f(t)) & 2(h_{20} + h_2 f(t)) & -(\omega_{22}^2 + \omega_2^2 f(t)) & -2(h_{22} + h_2 f(t)) \end{bmatrix} \tag{8}$$

The $\hat{A}(t)$ matrix is a periodic matrix according to the model in question, which means that it is a matrix with periodic functions of time.

$$\hat{A}(t + 2\pi/\omega) = \hat{A}(t) \text{ or } \hat{A}(t + T) = \hat{A}(t) \tag{9}$$

Based on the analysis of the above-mentioned works on parametric equations, we can conclude that complex systems (for example, the printing unit) are expected to contain areas of instability. In the case of the presented parametric system, the areas of instability should be sought for the parameters satisfying the following conditions:

$$\omega = \frac{2\Omega_i}{n}, n = 1, 2, 3, ..., .i = 1, 2 \tag{10}$$

$$\omega = \frac{|\Omega_1 \pm \Omega_2|}{n}, n = 1, 2, 3, ..., \tag{11}$$

where Ω_i—natural frequency of the system.

Such resonances (11) are known as combination parametric resonances of the summation and differential type [18,50].

The question is what should be regarded as the natural frequency of the system, if stiffness and viscosity of the system changes periodically? Stiffness and viscosity should be replaced by averaged values when calculating the natural frequencies of the system. The quality of averaged values takes the first part of the Fourier series $k\ a_0/2, c\ a_0/2$ [27].

To determine the natural frequencies of the system, where stiffness and damping change periodically, Eq. (1) was replaced by the averaged equation

$$\dot{z}(t) = \hat{A}_0 \mathbf{z}(t) \tag{12}$$

where $\hat{A}_0 = T^{-1} \int_0^T \hat{A}(t)\, dt$. It should be taken into account that the $\hat{A}_0$ matrix is a matrix with constant coefficients, i.e. the $\hat{A}(t)$ matrix contains the $a_0/2$ parameter instead of the function $f(t)$.

After taking into account the formula (5), we can calculate the a_0 coefficient

$$a_0 = \frac{2}{T}\left(\int_0^{T-2\varepsilon-\varepsilon_0} f(t)\, dt + \int_{T-2\varepsilon-\varepsilon_0}^{T-\varepsilon-\varepsilon_0} f(t)\, dt + \int_{T-\varepsilon}^{T} f(t)\, dt\right) = 2\left(1 - \frac{(\varepsilon + \varepsilon_0)\omega}{2\pi}\right)$$

In the end, we obtain the following equation

$$\frac{a_0}{2} = 1 - \frac{\varepsilon + \varepsilon_0}{T} \tag{13}$$

For $\varepsilon = T/16, \varepsilon_0 = T/8 (2\varepsilon + \varepsilon_0 = T/4)$ the $a_0/2 = 13/16$ coefficient, for $\varepsilon = T/32, \varepsilon_0 = 3T/16$, $(2\varepsilon + \varepsilon_0 = T/4)$ the $a_0/2 = 25/32$ coefficient, for $\varepsilon = T/64, \varepsilon_0 = 7T/32\ (2\varepsilon + \varepsilon_0 = T/4)$ the $a_0/2 = 49/64$ coefficient. Conclusion: with the reduction of the εparameter, the a_0 coefficient decreases at fulfilling the condition $2\varepsilon + \varepsilon_0 = T/4$.

3 The analysis of stability areas of processes occurring in the printing unit model

The instability areas of the presented parametric system should be sought for parameters satisfying the following conditions: (10) and (11). We will expand the function $f(t)$ in a Fourier series (14) in the $[0, T]$ interval, where $T = 2\pi/\omega$ [51].

$$f(t) = \frac{a_0}{2} + \sum_{n=1}^{\infty} (a_n \cos(n\omega t) + b_n \sin(n\omega t)) \tag{14}$$

where

$$a_0 = \frac{2}{T}\int_0^T f(t)\,dt,\ a_n = \frac{2}{T}\int_0^T f(t)\cos(n\omega t)dt,\ b_n = \frac{2}{T}\int_0^T f(t)\sin(n\omega t)dt \tag{15}$$

Formally, we obtain $a_{-n} = a_n, b_{-n} = -b_n, b_0 = 0$.

After taking into account the formula (5), we can calculate coefficients a_n, b_n. Finally, we obtain

$$a_n = \frac{3T^3}{2\varepsilon^3 n^4\pi^4}\left(1 - \cos\theta_0 - \cos\theta_1 + \cos\theta_2 + \frac{\varepsilon}{T}n\pi(\sin\theta_0 - \sin\theta_1 - \sin\theta_2)\right)$$

$$b_n = \frac{3T^3}{2\varepsilon^3 n^4\pi^4}\left(-\sin\theta_0 - \sin\theta_1 + \sin\theta_2 - \frac{\varepsilon}{T}n\pi(1 + \cos\theta_0 - \cos\theta_1 - \cos\theta_2)\right) \tag{16}$$

where

$$\theta_0 = \frac{2n\pi(T-\varepsilon)}{T},\ \theta_1 = \frac{2n\pi(T-\varepsilon-\varepsilon_0)}{T},\ \theta_2 = \frac{2n\pi(T-2\varepsilon-\varepsilon_0)}{T}$$

We can write the approximating series for the N elements

$$f(t) = \frac{a_0}{2} + \sum_{n=1}^{N}\left(a_n \cos\left(\frac{n2\pi t}{T}\right) + b_n \sin\left(\frac{n2\pi t}{T}\right)\right) \tag{17}$$

It was required to use the method of generalized Hill's determinants to obtain critical parameters of a parametric resonance (a condition for the stability of periodic vibrations). In accordance with the Floquet theory, this method uses the fact that there is a particular solution of the (1) equation:

$$\mathbf{z}(t) = e^{st}\chi(t) \tag{18}$$

where $\chi(t)$—periodic vector. The idea of that method is based on searching for a vector-function $\chi(t)$ in the form of a Fourier series with vector coefficients of the vector. As a result, we can solve the equation by the s coefficient. This equation is the result of a generalized Hill's determinant for the theory of Mathieu-Hill equation.

Using the expanded function (14), we can write the $\hat{A}(t)$ matrix in the following form

$$\hat{A}(t) = \hat{A}_0 + \sum_{n=1}^{\infty}\left(\hat{A}_n\cos(n\omega t) + \hat{B}_n\sin(n\omega t)\right) \tag{19}$$

where matrices

$$\hat{A}_0 = \begin{bmatrix} 0 & 1 & 0 & 0 \\ -(\omega_{11}^2 + 0.5\omega_1^2 a_0) & -(2h_{11} + h_1 a_0) & \omega_{10}^2 + 0.5\omega_1^2 a_0 & 2h_{10} + h_1 a_0 \\ 0 & 0 & 0 & 1 \\ \omega_{20}^2 + 0.5\omega_2^2 a_0 & 2h_{20} + h_2 a_0 & -(\omega_{22}^2 + 0.5\omega_2^2 a_0) & -(2h_{22} + h_2 a_0) \end{bmatrix} \tag{20}$$

$$\hat{A}_n = \begin{bmatrix} 0 & 0 & 0 & 0 \\ -\omega_1^2 a_n & -2h_1 a_n & \omega_1^2 a_n & 2h_1 a_n \\ 0 & 0 & 0 & 0 \\ \omega_2^2 a_n & 2h_2 a_n & -\omega_2^2 a_n & -2h_2 a_n \end{bmatrix} \tag{21}$$

$$\hat{B}_n = \begin{bmatrix} 0 & 0 & 0 & 0 \\ -\omega_1^2 b_n & -2h_1 b_n & \omega_1^2 b_n & 2h_1 b_n \\ 0 & 0 & 0 & 0 \\ \omega_2^2 b_n & 2h_2 b_n & -\omega_2^2 b_n & -2h_2 b_n \end{bmatrix} \tag{22}$$

have fixed coefficients.

The $\hat{A}_0$ matrix is non-singular and has an inverse matrix $\hat{A}_0^{-1}$. The vector state $\mathbf{z}(t)$ should be expanded in the Fourier series with vector coefficients of vector

$$\mathbf{z}(t) = \exp(st)\left[\frac{1}{2}\mathbf{Z}_0 + \sum\nolimits_{k=1}^{\infty}(\mathbf{Z}_k \cos k\omega t + \mathbf{Y}_k \sin k\omega t)\right] \tag{23}$$

We can substitute the equation (1) with (19) and (23). For this purpose, we will use the theory of Fourier series. By equating coefficients to zero at the same $\exp(st)\cos(k\omega t)$ and $\exp(st)\sin(k\omega t)$ we obtain homogeneous systems of linear algebraic equations for the components of $\mathbf{Z}_k$ and $\mathbf{Y}_k$ vectors

$$\begin{cases} \left(\hat{A}_0 - s\hat{I}\right)\mathbf{Z}_k + \frac{1}{2}\sum\limits_{m=1}^{\infty}\left(\hat{A}_m(\mathbf{Z}_{m+k} + \mathbf{Z}_{m-k}) + \hat{B}_m(\mathbf{Y}_{m+k} + \mathbf{Y}_{m-k})\right) = \omega k\mathbf{Y}_k \\ (\hat{A}_0 - s\hat{I})\mathbf{Z}_0 + \sum\limits_{m=1}^{\infty}\left(\hat{A}_m\mathbf{Z}_m + \hat{B}_m\mathbf{Y}_m\right) = 0 \\ \left(\hat{A}_0 - s\hat{I}\right)\hat{Y}_k + \frac{1}{2}\sum\limits_{m=1}^{\infty}\left(\hat{A}_m(\mathbf{Y}_{m+k} - \mathbf{Y}_{m-k}) - \hat{B}_m(\mathbf{Z}_{m+k} - \mathbf{Z}_{m-k})\right) = -\omega k\mathbf{Z}_k \end{cases} \tag{24}$$

The system of equations can also be written as follows

$$\begin{bmatrix} \ddots & \cdots & \cdots & \cdots & \cdots & \cdots & \iddots \\ \vdots & \widehat{\mathbf{A}}_0 - s\widehat{\mathbf{I}} + 0.5\widehat{\mathbf{A}}_4 & 0.5(\widehat{\mathbf{A}}_3 + \widehat{\mathbf{A}}_1) & 0.5\widehat{\mathbf{A}}_2 & 0.5(\widehat{\mathbf{B}}_3 - \widehat{\mathbf{B}}_1) & -2\omega\widehat{\mathbf{I}} + 0.5\widehat{\mathbf{B}}_4 & \vdots \\ \vdots & 0.5(\widehat{\mathbf{A}}_1 + \widehat{\mathbf{A}}_3) & \widehat{\mathbf{A}}_0 - s\widehat{\mathbf{I}} + 0.5\widehat{\mathbf{A}}_2 & 0.5\widehat{\mathbf{A}}_1 & 0.5\widehat{\mathbf{B}}_2 - \omega\widehat{\mathbf{I}} & 0.5(\widehat{\mathbf{B}}_1 + \widehat{\mathbf{B}}_3) & \vdots \\ \vdots & \widehat{\mathbf{A}}_2 & \widehat{\mathbf{A}}_1 & \widehat{\mathbf{A}}_0 - s\widehat{\mathbf{I}} & \widehat{\mathbf{B}}_1 & \widehat{\mathbf{B}}_2 & \vdots \\ \vdots & 0.5(\widehat{\mathbf{B}}_3 - \widehat{\mathbf{B}}_1) & \omega\widehat{\mathbf{I}} + 0.5\widehat{\mathbf{B}}_2 & 0.5\widehat{\mathbf{B}}_1 & \widehat{\mathbf{A}}_0 - s\widehat{\mathbf{I}} - 0.5\widehat{\mathbf{A}}_2 & 0.5(\widehat{\mathbf{A}}_1 - \widehat{\mathbf{A}}_3) & \vdots \\ \vdots & 2\omega\widehat{\mathbf{I}} + 0.5\widehat{\mathbf{B}}_4 & 0.5(\widehat{\mathbf{B}}_3 + \widehat{\mathbf{B}}_1) & 0.5\widehat{\mathbf{B}}_2 & 0.5(\widehat{\mathbf{A}}_1 - \widehat{\mathbf{A}}_3) & \widehat{\mathbf{A}}_0 - s\widehat{\mathbf{I}} - 0.5\widehat{\mathbf{A}}_4 & \vdots \\ \iddots & \cdots & \cdots & \cdots & \cdots & \cdots & \ddots \end{bmatrix} \begin{bmatrix} \vdots \\ \mathbf{Z}_2 \\ \mathbf{Z}_1 \\ \mathbf{Z}_0 \\ \mathbf{Y}_1 \\ \mathbf{Y}_2 \\ \vdots \end{bmatrix} = 0 \tag{25}$$

The nontrivial solution of the system of linear algebraic equations for the components of $\mathbf{Z}_k$ and $\mathbf{Y}_k$ vectors exists for $\det\left(\hat{H} - s\hat{I}\right) = 0$, where $\hat{H}$—an infinite block matrix.

The dimension of the phase space is equal to $n = 4$ for the considered model. The $\hat{H}$ matrix is $n(2m + 1) = 28$ when maintaining $m = 3$ in the Fourier series

$$\widehat{\mathbf{H}} = \begin{bmatrix} \widehat{\mathbf{A}}_0 + 0.5\widehat{\mathbf{A}}_6 & 0.5(\widehat{\mathbf{A}}_5 + \widehat{\mathbf{A}}_1) & 0.5(\widehat{\mathbf{A}}_4 + \widehat{\mathbf{A}}_2) & 0.5\widehat{\mathbf{A}}_3 & 0.5(\widehat{\mathbf{B}}_4 - \widehat{\mathbf{B}}_2) & 0.5(\widehat{\mathbf{B}}_5 - \widehat{\mathbf{B}}_1) & 0.5\widehat{\mathbf{B}}_6 - 3\omega\widehat{\mathbf{I}}) \\ 0.5(\widehat{\mathbf{A}}_5 + \widehat{\mathbf{A}}_1) & \widehat{\mathbf{A}}_0 + 0.5\widehat{\mathbf{A}}_4 & 0.5(\widehat{\mathbf{A}}_3 + \widehat{\mathbf{A}}_1) & 0.5\widehat{\mathbf{A}}_2 & 0.5(\widehat{\mathbf{B}}_3 - \widehat{\mathbf{B}}_1) & 0.5\widehat{\mathbf{B}}_4 - 2\omega\widehat{\mathbf{I}} & 0.5(\widehat{\mathbf{B}}_5 + \widehat{\mathbf{B}}_1) \\ 0.5(\widehat{\mathbf{A}}_4 + \widehat{\mathbf{A}}_2) & 0.5(\widehat{\mathbf{A}}_1 + \widehat{\mathbf{A}}_3) & \widehat{\mathbf{A}}_0 + 0.5\widehat{\mathbf{A}}_2 & 0.5\widehat{\mathbf{A}}_1 & 0.5\widehat{\mathbf{B}}_2 - \omega\widehat{\mathbf{I}} & 0.5(\widehat{\mathbf{B}}_1 + \widehat{\mathbf{B}}_3) & 0.5(\widehat{\mathbf{B}}_4 + \widehat{\mathbf{B}}_2) \\ \widehat{\mathbf{A}}_3 & \widehat{\mathbf{A}}_2 & \widehat{\mathbf{A}}_1 & \widehat{\mathbf{A}}_0 & \widehat{\mathbf{B}}_1 & \widehat{\mathbf{B}}_2 & \widehat{\mathbf{B}}_3 \\ 0.5(\widehat{\mathbf{B}}_4 - \widehat{\mathbf{B}}_2) & 0.5(\widehat{\mathbf{B}}_3 - \widehat{\mathbf{B}}_1) & 0.5\widehat{\mathbf{B}}_2 + \omega\widehat{\mathbf{I}} & 0.5\widehat{\mathbf{B}}_1 & \widehat{\mathbf{A}}_0 - 0.5\widehat{\mathbf{A}}_2 & 0.5(\widehat{\mathbf{A}}_1 - \widehat{\mathbf{A}}_3) & 0.5(\widehat{\mathbf{A}}_2 - \widehat{\mathbf{A}}_4) \\ 0.5(\widehat{\mathbf{B}}_5 - \widehat{\mathbf{B}}_1) & 0.5\widehat{\mathbf{B}}_4 + 2\omega\widehat{\mathbf{I}} & 0.5(\widehat{\mathbf{B}}_3 + \widehat{\mathbf{B}}_1) & 0.5\widehat{\mathbf{B}}_2 & 0.5(\widehat{\mathbf{A}}_1 - \widehat{\mathbf{A}}_3) & \widehat{\mathbf{A}}_0 - 0.5\widehat{\mathbf{A}}_4 & 0.5(\widehat{\mathbf{A}}_1 - \widehat{\mathbf{A}}_5) \\ 0.5\widehat{\mathbf{B}}_6 + 3\omega\widehat{\mathbf{I}}) & 0.5(\widehat{\mathbf{B}}_5 + \widehat{\mathbf{B}}_1) & 0.5(\widehat{\mathbf{B}}_4 + \widehat{\mathbf{B}}_2) & 0.5\widehat{\mathbf{B}}_3 & 0.5(\widehat{\mathbf{A}}_2 - \widehat{\mathbf{A}}_4) & 0.5(\widehat{\mathbf{A}}_1 - \widehat{\mathbf{A}}_5) & \widehat{\mathbf{A}}_0 - 0.5\widehat{\mathbf{A}}_6 \end{bmatrix} \tag{26}$$

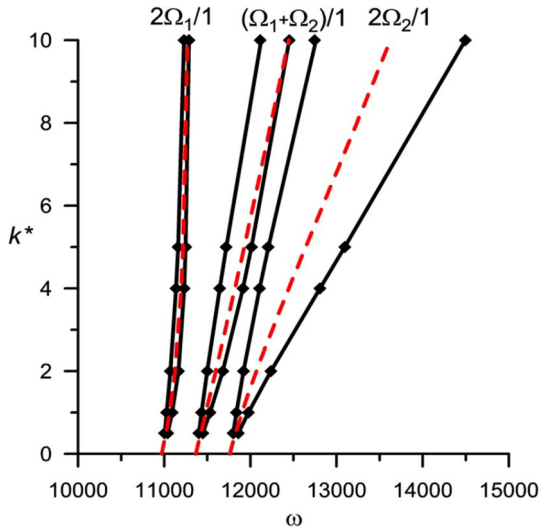

Fig. 4 The areas of stability of the Hill equation (1) with periodic coefficients determined according to (5) for $n = 1$

To calculate the instability area in the vicinity of the lateral resonance of order n, it is necessary to leave harmonics to the order n in series (19) and (23).

When solving an algebraic equation of the 28 series $\det\left(\hat{H} - s\hat{I}\right) = 0$ according to the s parameter, we should define the k^* and ω parameter values, for which the elements have a positive real part.

We will carry out a numerical analysis of parameters [2,3]: $m_1 = 85\,\text{kg}$, $m_2 = 105\,\text{kg}$, $k_1 = 2.94\times 10^9$ N m^{-1}, $k_2 = 3.16\times 10^9$ N m^{-1}, $k_{12} = 0$, $k = k^*\times 10^8$N m^{-1}, $c_1 = c_2 = 4.9\times 10^2$ N s^2 m^{-1}, $c_{12} = 0$, $c = 9.21\times 10^2$ N s^2 m^{-1}. We conducted a numerical analysis for the dimensionless parameter (modulation depth) k^* = 0.5; 1.0; 2.0; 4.0; 5.0; 6.0; 10.0 associated with changing stiffness of the blanket. This choice is made to cover a wide range of scenarios from practical applications. At the same time, numerical simulations are performed for different frequencies ω [s^{-1}]. The areas of parametric resonance are shown in the following figures (Figs. 4, 5, 6 and 7). These areas are located between two curves (boundaries of the stability area) and combine frequencies calculated by the Eqs. (10) and (11) for different values of n.

The areas known as tongues of instability determine the modulation depth and frequency of ω changes, for which the state of inaction loses stability. The induced vibrations have a frequency that is close to the frequency specified by formulas (10) and (11) at low modulation depth.

Figure 4 shows the areas of parametric resonance for $n = 1$. Three areas of parameter values k^* and ω [s^{-1}], for which there is a parametric resonance, combine corresponding values $2\Omega_2$ /1, $(\Omega_1 + \Omega_2)$/1, $2\Omega_1$/1. For example, there is a lack of parametric resonance for $k^* = 0.0$; $\Omega_1 = 5485.93\text{s}^{-1}$, $\Omega_2 = 5881.15\text{s}^{-1}$. For $k^* = 0.5$, $\omega \in [11006, 11040]$, $\omega \in [11402, 11449]$, $\omega \in [11801, 11860]$ we obtain a parametric resonance, $\Omega_1 = 5511.15\text{s}^{-1}$; $\Omega_2 = 5914.85\text{s}^{-1}$.

The areas of critical parameters k^* and ω have also been calculated according to the above method. The critical parameters are calculated from the condition (Re s_j), where s_j—roots of the equation $\det(\hat{H} - s\hat{I}) = 0$. The determinant equation $\det(\hat{H} - s\hat{I}) = 0$ was solved using function *Eigenvalues*$[\hat{H}]$ system Wolfram Mathematica. The values of k^* and ω parameters are shown in Fig. 4 in the form of points. As can be seen from Fig. 4, the computational simulation and analytical approach give the same results for the considered parameters. For example, the numerical simulation in the worst case scenario gives the following area of instability for $k^* = 10$, $\omega \in [12762, 14495]$, $(2\Omega_2$ /1 $\in [12762, 14495])$. Theoretical calculations give the following area $\omega \in [12745, 14496]$. The areas of instability for higher n parameters will be slightly different when analysing the areas of instability in values (10) and (11). The analytical approach may not be capable of calculating certain areas of instability for higher n parameters. In that case, one has to increase the dimension of the $\hat{H}$ matrix.

Figure 5 shows areas of parametric resonance for $n = 2$. The three areas of parameter values k^* and ω, for which there is a parametric resonance and which include the appropriate values $2\Omega_2$ /2, $(\Omega_1 + \Omega_2)$/2, $2\Omega_1$ /2, are the same.

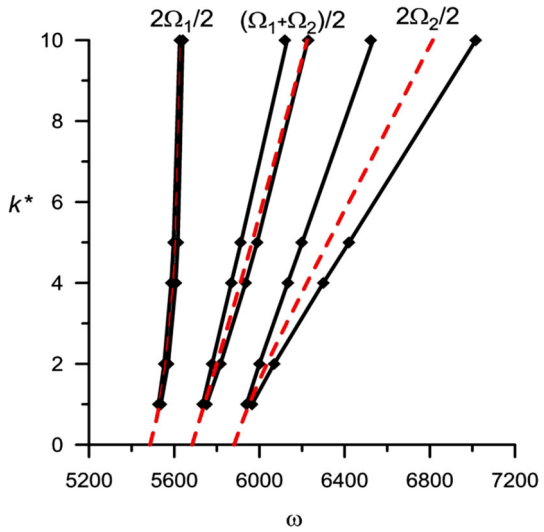

Fig. 5 The areas of stability of the Hill equation (1) with periodic coefficients determined according to (5) for $n = 2$

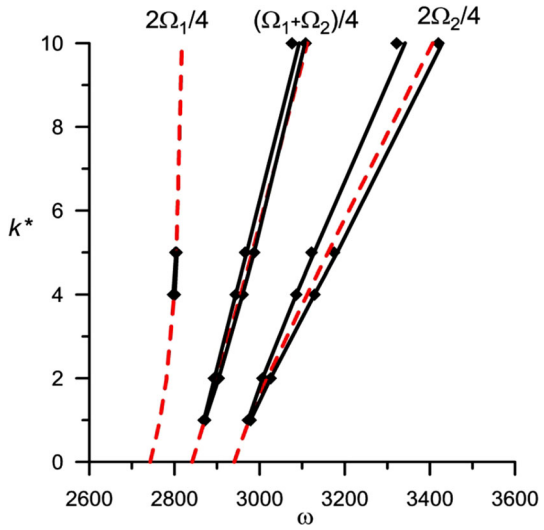

Fig. 6 The areas of stability of the Hill equation (1) with periodic coefficients determined according to (5) for $n = 4$

For example, for $k^* = 0.0$ and $k^* = 0.5$ there is a lack of parametric resonance. For $k^* = 1.0$, $\omega \in [5526, 5537]$, $\omega \in [5733, 5751]$, $\omega \in [5939, 5965]$ we obtain a parametric resonance $\Omega_1 = 5511.15\text{s}^{-1}$; $\Omega_2 = 5914.85\text{s}^{-1}$.

Figure 6 shows areas of parametric resonance for $n = 4$. It can be seen that the area of parameter instability exists only for $k^* = 4.0$, $\omega \in [2797, 2801]$ and for $k^* = 5.0$, $\omega \in [2803, 2806]$.

Figure 7 shows areas of parametric resonance for $n = 5$. The area of parameters for the value $(\Omega_1 + \Omega_2)/5$ for $k^* > 7$ is shifted towards lower values ω.

It can be seen that for $k^* = 10$, the values calculated according to the analytical approach are lower than the values obtained during the computational simulation. For example, the computational simulation gives values $\omega \in [2242, 2265]$, $\omega \in [2472, 2486]$, $\omega \in [2666, 2746]$, and calculations according to the analytical approach give the following values: $\omega \in [2455, 2485]$, $\omega \in [2651, 2731]$. In the worst case, this constitutes 0.7%. However, it should be noted that we cannot calculate the area of instability using the analytical approach (Fig. 7 does not show any points from analytical calculations).

The total stiffness of the system increases when the system gets equipped with bearer rings ($k_{12} = 5.09 \times 10^9$ N m^{-1}). The natural frequencies of the modified system are $\Omega_1 = 5662.25$ s^{-1} and $\Omega_2 = 12044.6$ s^{-1}. In this case, one cannot observe any parametric resonance [27].

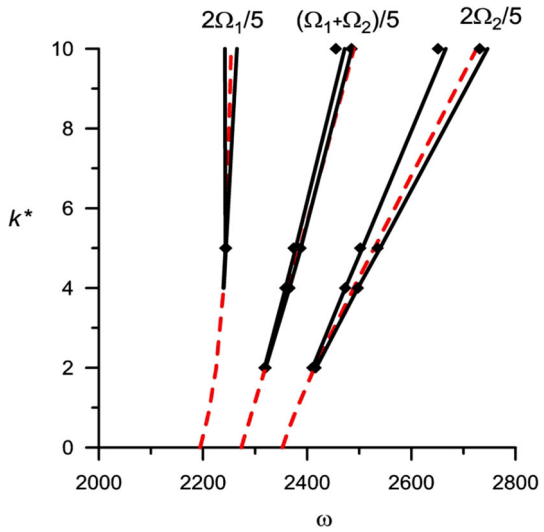

Fig. 7 The areas of stability of the Hill equation (1) with periodic coefficients determined according to (5) for $n = 5$

4 Conclusion

The paper presents a model of parametric vibrations in the system associated with the printing machine.

The periodically changing stiffness of the system was modelled.

The analysis of the proposed model is reduced to solving a set of Hill equations.

The peculiarity of the obtained equations is the relationship between the natural frequencies of the system and modulation depth.

It was required to use a numerical simulation and the method of generalized Hill's determinants to obtain critical parameters of a parametric resonance.

Parametric resonances can occur within the system that is not equipped with bearer rings ($k_{12} = 0$) only when conditions (10) and (11) are met (Figs. 4, 5, 6 and 7). Conversely, when $k_{12} > 0$, i.e., when cylinders are equipped with bearer rings,[24] the stiffness of the system increases to a level at which the parametric resonance may not occur.

As a future development, using the preliminary results presented here, we can design the elastic connections between the cylinders and the ground using metamaterials instead of conventional links. Specifically, metamaterials can be designed with specific internal structures that dissipate energy and reduce the transmission of shock waves. Some common structures for doing that include: (1) *Auxetic Metamaterials*: these have a negative Poisson's ratio, meaning they become thicker perpendicular to the applied force [52]. This can enhance their ability to absorb and dissipate energy. (2) *Lattice Structures*: these are periodic arrangements of beams or struts that can deform in specific ways to absorb energy [53,54]. (3) *Multilayered Metamaterials*: layers of materials with different mechanical properties can reflect and absorb shock waves more effectively than a single layer [55–59]. Moreover, advanced manufacturing techniques are often used to create the complex structures required for metamaterials: (i) 3D Printing (Additive Manufacturing): allows for precise control over the internal structure and can create intricate designs not possible with traditional manufacturing. (ii) Laser Cutting and Etching: useful for creating detailed patterns in thin sheets of material. (iii) Microfabrication: techniques used in semiconductor manufacturing can create very fine structures at small scales. The properties of metamaterials can be tuned by altering their geometry and structure. Parameters such as unit cell size, shape, and arrangement can be adjusted to achieve the desired level of shock absorption. In the considered application, particular attention must be paid to dynamic performances [60–66]. Among them, the tuning of proper bang gaps is of the utmost importance [67–70]. Moreover, microstructure causes nonlocality in vibrations [71] that changes the inertia of the overall system [72]. Cyclic mechanical vibrations may lead to fatigue related damage [73].

Finally, inverse analysis is needed for nonlinear viscoelastic material models [74].

Acknowledgements This study was accomplished under the research project No. 2011/03/B/ST8/06478, which was financed by the National Science Centre, Poland.

Funding Open access funding provided by Università degli Studi dell'Aquila within the CRUI-CARE Agreement. The author disclosed receipt of the following financial support for the research, authorship, and/or publication of this article: This research received financial support from the Institute of Mechanics and Printing.

Declarations

Conflict of interest The author declared no potential Conflict of interest with respect to the research, authorship, and/or publication of this article.

References

1. Kipphan, H.: Handbook of Print Media. Technologies and Production Methods. Springer-Verlag, Berlin Heidelberg (2001)
2. Kulikov, G.B.: Diagnosing causes of increased vibration of printing units of tower rotary printing presses. J. Mach. Manuf. Reliab. **37**(4), 391–396 (2008)
3. Gao, X.: Schwingungen von Offsetdruckmaschienen. Master Dissertation, TU Chemnitz, (2001)
4. Augustaitis, V.K., Šešok, N.: Analytical investigation of transversal vibrations of and plate cylinder of offset printing press. Mechanika **1**(13), 46–53 (2000)
5. Lei, X., Hou, H., Zha, Z., Liu, S., Xu, B., Liu, P.: Dynamic characteristics of printing cylinder with rotating dynamic load. Math. Models Eng. **6**(1), 50–56 (2020)
6. Šešok, N., Iljin, I.: The investigation on the impact of the contact rings of cylinders and on transversal vibrations of blanket and plate cylinders in offset printing press. J. Vibroeng. **12**(1), 95–100 (2010)
7. Hou, H.P., Rui, T.T., Deng, R., Xu, Z.F., Liu, S.H.: Modal analysis of central impression cylinder based on fluid-solid coupling method. J. Low Freq. Noise Vib. Active Control **40**(1), 772–783 (2021)
8. Hermanski, M., Kohn, K.U., Ostholt, H.: An adaptive spectral compensation algorithm for avoiding flexural vibration of printing cylinders. J. Sound Vib. **185**(1), 185–193 (1995)
9. Augustaitis, V.K., Šešok, N.: Elimination of the relative deflections of cylinders of lithographic web press. Mechanika **6**(38), 28–35 (2002)
10. Augustaitis, V.K., Šešok, N.: Relative transversal vibrations of printing—press cylinders that are pressed against each other via an elastic blanket. Strojniški Vestnik J. Mech. Eng. **50**(3), 277–290 (2004)
11. Augustaitis, V.K., Šešok, N., Iljin, I.: Impact of contact rings in plate and blanket cylinders of printing section's drive on its dynamic accuracy. Mechanika **61**(3), 38–45 (2006)
12. Messer, M.H.E.: Parametric excitation of vibrations in printing machines. Int. J. Acoust. Vib. **22**(4), 448–455 (2017)
13. Razinkin, E.V.: Method for Calculation of Dynamical Parameters of Tower Printing Machines. Extended Abstract of Cand. Sci. (Eng.) Dissertation. Moscow, Moscow State Printing Inst (2006)
14. Greco, D., Blanc, P., Aubry, E., et al.: Active vibration control of flexible materials found within printing machines. J. Sound Vib. **300**(3–5), 831–846 (2007)
15. Destree, T.: Guide to Troubleshooting for the Sheetfed Offset Press. COBRPP, Warsaw (2007)
16. Yamaguchi, M., Takasaki, K., Hirooka, H., et al.: Development of dynamic absorber built-in roll for high-speed and high-quality sheet-fed offset printing press. Mitsubishi Heavy Ind. Tech. Rev. **34**(1), 20–24 (1997)
17. Den Hartog, J.R.: Mechanical Vibrations. McGraw-Hill, New York (1956)
18. Bolotin, V.V.: The Dynamic Stability of Elastic Systems. Holden-Day, San Francisco (1964)
19. Osiński, Z.: Theory of Vibrations. PWN, Warsaw (1980)
20. Awrejcewicz, J.: Oscillations of Lumped Deterministic System. WNT, Warsaw (1996)
21. Giergiel, J.: Damping of Mechanical Vibrations. PWN, Warsaw (1990)
22. Pyryev, Y., Krzyżkowski, J.: Parametric vibrations in printing unit of offset printing machine. Vib. Phys. Syst. **25**, 335–340 (2012)
23. Yakubovich, V.A., Starzhinskii, V.M.: Linear differential equations with periodic coefficients, vol. 2. Wiley, New York (1975)
24. Krzyżkowski, J., Pyryev, Y.: Construction of cylinders in offset printing presses and its vibratory consequences. Chall. Mod. Technol. **3**(1), 15–18 (2012)
25. Krzyżkowski, J., Pyryev, Y.: Cylinder gap shock and its impact on quality of prints in offset printing technique. Chall. Mod. Technol. **4**(1), 23–30 (2013)
26. Krzyżkowski, J., Pyryev, Y.: Spectral analysis of parametric two degrees- of-freedom system. Chall. Mod. Technol. **6**(4), 8–13 (2015)
27. Pyryev, Y., Krzyżkowski, J.: Parametric vibrations in offset printing units. Theor. Appl. Mech. Lett. (TAML) **2**(4), 043011 (2012)
28. Kodinskiy, A.I.: The influence of backlash in the bearings of the printing machine to print quality. Probl. Print. Publ. **4**, 19–29 (2004)

29. dell'Isola, F., Seppecher, P., Alibert, J.J., et al.: Pantographic metamaterials: an example of mathematically driven design and of its technological challenges. Contin. Mech. Thermodyn. **31**, 851–884 (2019)
30. dell'Isola, F., Seppecher, P., Spagnuolo, M., et al.: Advances in pantographic structures: design, manufacturing, models, experiments and image analyses. Contin. Mech. Thermodyn. **31**, 1231–1282 (2019)
31. Barchiesi, E., Spagnuolo, M., Placidi, L.: Mechanical metamaterials: a state of the art. Math. Mech. Solids **24**(1), 212–234 (2019)
32. Giorgio, I., Spagnuolo, M., Andreaus, U., et al.: In-depth gaze at the astonishing mechanical behavior of bone: a review for designing bio-inspired hierarchical metamaterials. Math. Mech. Solids **26**(7), 1074–1103 (2021)
33. Abali, B.E.: Revealing the physical insight of a length-scale parameter in metamaterials by exploiting the variational formulation. Contin. Mech. Thermodyn. **31**(4), 885–894 (2019)
34. dell'Isola, F., Misra, A.: Principle of virtual work as foundational framework for metamaterial discovery and rational design. Comptes Rendus Mécanique **351**(S3), 1–25 (2023)
35. Aydin, G., Sarar, B.C., Yildizdag, M.E., Abali, B.E.: Investigating infill density and pattern effects in additive manufacturing by characterizing metamaterials along the strain-gradient theory. Math. Mech. Solids **27**(10), 2002–2016 (2022)
36. dell'Isola, F., Lekszycki, T., Pawlikowski, M., Grygoruk, R., Greco, L.: Designing a light fabric metamaterial being highly macroscopically tough under directional extension: first experimental evidence. Z. Angew. Math. Phys. **66**, 3473–3498 (2015)
37. Yang, H., Ganzosch, G., Giorgio, I., Abali, B.E.: Material characterization and computations of a polymeric metamaterial with a pantographic substructure. Z. Angew. Math. Phys. **69**, 1–16 (2018)
38. Yildizdag, M. E., Tran, C. A., Barchiesi, E., Spagnuolo, M., dell'Isola, F., Hild, F.: A multi-disciplinary approach for mechanical metamaterial synthesis: a hierarchical modular multiscale cellular structure paradigm. State of the art and future trends in material modeling, pp. 485–505 (2019)
39. Eugster, S.R., dell'Isola, F., Fedele, R., Seppecher, P.: Piola transformations in second-gradient continua. Mech. Res. Commun. **120**, 103836 (2022)
40. Turco, E., Barchiesi, E., Causin, A., dell'Isola, F., Solci, M.: Kresling tube metamaterial exhibits extreme large-displacement buckling behavior. Mech. Res. Commun. **134**, 104202 (2023)
41. Carcaterra, A., dell'Isola, F., Esposito, R., Pulvirenti, M.: Macroscopic description of microscopically strongly inhomogenous systems: a mathematical basis for the synthesis of higher gradients metamaterials. Arch. Ration. Mech. Anal. **218**, 1239–1262 (2015)
42. Misra, A., Lekszycki, T., Giorgio, I., Ganzosch, G., Müller, W.H., dell'Isola, F.: Pantographic metamaterials show atypical Poynting effect reversal. Mech. Res. Commun. **89**, 6–10 (2018)
43. Giorgio, I., Hild, F., Gerami, E., dell'Isola, F., Misra, A.: Experimental verification of 2D Cosserat chirality with stretch-micro-rotation coupling in orthotropic metamaterials with granular motif. Mech. Res. Commun. **126**, 104020 (2022)
44. Spagnuolo, M., Andreaus, U., Misra, A., Giorgio, I., Hild, F.: Mesoscale modeling and experimental analyses for pantographic cells: effect of hinge deformation. Mech. Mater. **160**, 103924 (2021)
45. Turco, E.: How the properties of pantographic elementary lattices determine the properties of pantographic metamaterials. New achievements in continuum mechanics and thermodynamics: a tribute to Wolfgang H. Müller, pp. 489–506 (2019)
46. Ciallella, A., D'Annibale, F., Del Vescovo, D., Giorgio, I.: Deformation patterns in a second-gradient lattice annular plate composed of "spira mirabilis" fibers. Contin. Mech. Thermodyn. **35**(4), 1561–1580 (2023)
47. Chen, Y.L., Ma, L.: A minimalist elastic metamaterial with meta-damping mechanism. Int. J. Solids Struct. (2024). https://doi.org/10.1016/j.ijsolstr.2024.112977
48. Del Vescovo, D., Giorgio, I.: Dynamic problems for metamaterials: review of existing models and ideas for further research. Int. J. Eng. Sci. **80**, 153–172 (2014)
49. Yildizdag, M.E., Ciallella, A., D'Ovidio, G.: Investigating wave transmission and reflection phenomena in pantographic lattices using a second-gradient continuum model. Math. Mech. Solids **28**(4), 1776–1789 (2023)
50. Schmidt, G.: Parametererregte Schwingungen. Deutscher Verl. der Wiss, Berlin (1975)
51. Korn, G.A., Korn, T.M.: Mathematical Handbook for Scientists and Engineers. McGraw-Hill, New York (1968)
52. Stilz, M., Plappert, D., Gutmann, F., Hiermaier, S.: A 3D extension of pantographic geometries to obtain metamaterial with semi-auxetic properties. Math. Mech. Solids **27**(4), 673–686 (2022)
53. Giorgio, I., dell'Isola, F., Steigmann, D.J.: Second-grade elasticity of three-dimensional pantographic lattices: theory and numerical experiments. Contin. Mech. Thermodyn. (2023). https://doi.org/10.1007/s00161-023-01240-w
54. Eugster, S., dell'Isola, F., Steigmann, D.: Continuum theory for mechanical metamaterials with a cubic lattice substructure. Math. Mech. Complex Syst. **7**(1), 75–98 (2019)
55. Ciallella, A., Giorgio, I., Barchiesi, E., et al.: A 3D pantographic metamaterial behaving as a mechanical shield: experimental and numerical evidence. Mater. Des. **237**, 112554 (2024)
56. Giorgio, I., Varano, V., dell'Isola, F., Rizzi, N.L.: Two layers pantographs: a 2D continuum model accounting for the beams' offset and relative rotations as averages in SO (2) Lie groups. Int. J. Solids Struct. **216**, 43–58 (2021)
57. Stilz, M., dell'Isola, F., Giorgio, I., Eremeyev, V.A., Ganzenmüller, G., Hiermaier, S.: Continuum models for pantographic blocks with second gradient energies which are incomplete. Mech. Res. Commun. **125**, 103988 (2022)
58. Yildizdag, M.E., Barchiesi, E., dell'Isola, F.: Three-point bending test of pantographic blocks: numerical and experimental investigation. Math. Mech. Solids **25**(10), 1965–1978 (2020)
59. Ciallella, A., La Valle, G., Vintache, A., Smaniotto, B., Hild, F.: Deformation mode in 3-point flexure on pantographic block. Int. J. Solids Struct. **265**, 112129 (2023)
60. Ciallella, A., Giorgio, I., Eugster, S.R., Rizzi, N.L., dell'Isola, F.: Generalized beam model for the analysis of wave propagation with a symmetric pattern of deformation in planar pantographic sheets. Wave Motion **113**, 102986 (2022)
61. Laudato, M., Manzari, L., Giorgio, I., Spagnuolo, M., Göransson, P.: Dynamics of pantographic sheet around the clamping region: experimental and numerical analysis. Math. Mech. Solids **26**(10), 1515–1537 (2021)
62. Shekarchizadeh, N., Laudato, M., Manzari, L., Abali, B.E., Giorgio, I., Bersani, A.M.: Parameter identification of a second-gradient model for the description of pantographic structures in dynamic regime. Z. Angew. Math. Phys. **72**(6), 190 (2021)

63. Ciallella, A., Pasquali, D., Gołaszewski, M., D'Annibale, F., Giorgio, I.: A rate-independent internal friction to describe the hysteretic behavior of pantographic structures under cyclic loads. Mech. Res. Commun. **116**, 103761 (2021)
64. Ciallella, A., D'Annibale, F., dell'Isola, F., Del Vescovo, D., Giorgio, I.: Modal analysis of a second-gradient annular plate made of an orthogonal network of logarithmic spiral fibers. In: Sixty Shades of Generalized Continua: Dedicated to the 60th Birthday of Prof. Victor A. Eremeyev, pp. 103–116. Cham: Springer International Publishing (2023)
65. Mancusi, G., Fabbrocino, F., Feo, L., Fraternali, F.: Size effect and dynamic properties of 2D lattice materials. Compos. B Eng. **112**, 235–242 (2017)
66. Cornacchia, F., Fabbrocino, F., Fantuzzi, N., Luciano, R., Penna, R.: Analytical solution of cross-and angle-ply nano plates with strain gradient theory for linear vibrations and buckling. Mech. Adv. Mater. Struct. **28**(5), 1201–1215 (2021)
67. El Sherbiny, M.G., Placidi, L.: Discrete and continuous aspects of some metamaterial elastic structures with band gaps. Arch. Appl. Mech. **88**, 1725–1742 (2018)
68. Nejadsadeghi, N., Placidi, L., Romeo, M., Misra, A.: Frequency band gaps in dielectric granular metamaterials modulated by electric field. Mech. Res. Commun. **95**, 96–103 (2019)
69. Placidi, L., El Sherbiny, M.G., Baragatti, P.: Experimental investigation for the existence of frequency band gap in a microstructure model. Math. Mech. Complex Syst. **9**(4), 413–421 (2022)
70. Placidi, L., Di Girolamo, F., Fedele, R.: Variational study of a Maxwell-Rayleigh-type finite length model for the preliminary design of a tensegrity chain with a tunable band gap. Mech. Res. Commun. **136**, 104255 (2024)
71. Mühlich, U., Abali, B.E., dell'Isola, F.: Commented translation of Erwin Schrödinger's paper 'On the dynamics of elastically coupled point systems' (Zur Dynamik elastisch gekoppelter Punktsysteme). Math. Mech. Solids **26**(1), 133–147 (2021)
72. Mandadapu, K.K., Abali, B.E., Papadopoulos, P.: On the polar nature and invariance properties of a thermomechanical theory for continuum-on-continuum homogenization. Math. Mech. Solids **26**(11), 1581–1598 (2021)
73. dell'Isola, F., Volkov, I.A., Igumnov, L.A., Eugster, S.R., Litvinchuk, S.Y., Kazakov, D.A., Gorohov, V.A., Abali, B.E.: Estimating fatigue related damage in alloys under block-type non-symmetrical low-cycle loading. New Achievements in Continuum Mechanics and Thermodynamics: A Tribute to Wolfgang H. Müller, pp. 81–92 (2019)
74. Abali, B.E., Wu, C.C., Müller, W.H.: An energy-based method to determine material constants in nonlinear rheology with applications. Contin. Mech. Thermodyn. **28**, 1221–1246 (2016)